J Fluoresc (2011) 21:1865–1870
DOI 10.1007/s10895-011-0881-8

ORIGINAL PAPER

Observations of the Effect of Confined Space on Fluorescence and Diffusion Properties of Molecules in Single Conical Nanopore Channels

Li-Xiang Zhang · Xiao-Hong Cao · Wei-Peng Cai · Yao-Qun Li

Received: 31 December 2010 / Accepted: 23 March 2011 / Published online: 30 March 2011

Abstract In this work, we investigated the fluorescence emission spectra and diffusion properties of dye molecules confined in different positions of conical nanopore channels using a laser scanning confocal fluorescence microscope. The results showed that a red shift of the emission spectra is observed from the tip section to the bottom section and the diffusion rate is slower in the channel than that in bulk solution, indicating a single conical nanopore channel can be used as a convenient tool for investigating the effect of confined space on the behaviors of molecules.

Keywords Nanostructures · Confinement · Fluorescence · Diffusion · Confocal laser scanning microscopy

Introduction

At present, fabrication and application of solid-state nanopores are becoming the focus of attention. Solid-state nanopores offer great flexibility in terms of shape, size and surface properties, as well as superior robustness compared with their biological counterparts. Artifical conical nanopore channel, where the bottom diameter of the pore is larger than its tip and a micro-nano channel is formed, exhibit unique properties including enhanced transport properties, lower resistance, improved sensor performance [1–3], and may serve as excellent experimental model systems for studying confinement of the pores. In confined space, fluid-fluid interactions interplay with fluid-wall interactions [4], and molecules confined within micro-nano scale geometrical restraints can exhibit behavior that is quite different from that observed in a bulk fluid. For example, the transport of a molecule with a size similar to that of the pore through which it is transported is known as hindered or restricted diffusion, and the effective diffusivity of a solute within a pore of comparable size is frequently found to be less than its value in bulk solution [5]. This phenomenon is of great importance in devices for controlled release of drugs and pesticides, ultrafiltration and other membrane techniques [6]. Most previous studies of chemistry in nanochannels and other nanostructures have been focused on DNA behavior [7–9], polymer conformation [10–12] and protein folding [13, 14]. Optical techniques such as fluorescence [15–17], UV-Vis [18, 19], IR [20] spectroscopy have been used to characterize nanochannel confinement. Because of the extremely small volume of the nanopore, it is still a challenging task to monitor physical or chemical processes occurring in the nanochannels.

In previous studies, fluorescence microscopy have been used to monitor localized functionalities of the glass nanopore surfaces [21, 22]. One way to study molecular behavior at nanoscale is to perform confocal laser scanning microscopy (CLSM). This technique can offer an opportunity to the localized detection of fluorescence. The ability of CLSM in optically sectioning thick samples makes it possible to acquire both cross-sectional (z) and orizontal section (xy) images at required depth directly from the intact glass conical nanopore channel. Besides, fluores-

L.-X. Zhang · X.-H. Cao · W.-P. Cai · Y.-Q. Li (✉)
Department of Chemistry
and Key Laboratory of Analytical Sciences,
College of Chemistry and Chemical Engineering,
Xiamen University,
Xiamen 361005, China
e-mail: yqlig@xmu.edu.cn

X.-H. Cao
Department of Applied Chemistry,
East China Institute of Technology,
Fuzhou 344000, China

cence recovery after photobleaching (FRAP) is a widely used technique in the quantitative analysis of diffusion characteristics of molecules in solution and cellular environments [23]. Therefore, the local diffusion can be determined from fluorescence recovery after photobleaching (FRAP).

In this work, we proposed that single conical nanopore channels could provide a platform to investigate the effect of confined space on the behaviors of molecules, making using of the varied spaces in a single conical channel. We investigated the fluorescence emission spectra and diffusion properties of dye molecules confined in different positions of conical nanopore channels using a laser scanning confocal fluorescence microscope. The results showed that a red shift of the emission spectra is observed from the tip section to the bottom section and the diffusion rate is slower in the channel than that in bulk solution, indicating a single conical nanopore channel can be used as a convenient tool for investigating the effect of confined space on the behaviors of molecules. The combination of single conical nanopore channels and laser scanning confocal fluorescence technique is very promising to discover new phenomena and characteristics of molecules in a confined space, and to study in situ physical or chemical reactions carried out in the confinement of a nanochannel.

Experimental Section

Chemicals and Materials Nile red (Acros Organics), Fluorescein isothiocyante (FITC, from Sigma-Aldrich), Rhodamine 6 G (R6G, from Merck), refractive index matching oil (n=1.51, from Leica-microsystems),H_2SO_4, H_2O_2, 15% $CaCl_2$, ethyl acetate, glycerol, Ferrocene (Fc, 99%, Alfa Aesar), Tetra-n-butylammonium hexafluorophosphate ($TBAPF_6$, 98%, Alfa Aesar), acetonitrile (Alfa Aesar). Prism glass capillary (1.35-mm outer diameter, 0.95-mm inner diameter, Hirschmann.), platinum wire (diameter 25 μm, from Alfa Aesar)

Preparation of Single Glass Conical Nanopore Channels and Determination of the Orifice Radius The single glass conical nanopore channels were prepared from glass capillaries according to the previous literature with slight modification [22, 24]. Firstly, the platinum wire was electrochemically etched in 15% $CaCl_2$ to obtain a sharpened tip. Afterwards, it was sealed into a glass capillary and the glass bottom was then polished until Pt was revealed (Pt nanodisk). Finally, the Pt sealed in glass was pulled out and etched to obtain single conical glass nanopore channels.

The radius of the pore is determined by measuring the steady-state diffusion-limited current of the Pt disk electrode prior to etching according to Eq. 1 [25],

$$i_d = 4nFDC_b r \quad (1)$$

where i_d is the steady-state limiting current of the nanodisk electrode measured in 5.0 mM Ferrocene and 0.1 M Tetra-n-butylammonium hexafluorophosphate acetonitrile solution, n is the number of electrons transferred per molecule, F is the Faraday constant, D is the diffusion coefficient (2.4×10^{-5} cm^2/s), C_b is bulk concentration of the redox molecule, and r is the radius of the Pt nanodisk, respectively. The half-cone angle and the depth of the pore can be determined from the confocal fluorescence image.

Confocal Laser Scanning Fluorescence Measurement We performed confocal imaging and confocal fluorescence measurements on an inverted confocal microscope (Leica TCS SP5, Leica Microsystems). The excitation source was an argon ion laser, wavelength 488 nm. 10× (NA 0.4) and a 20× (NA 0.7) objectives and a 100×(NA 1.4) oil

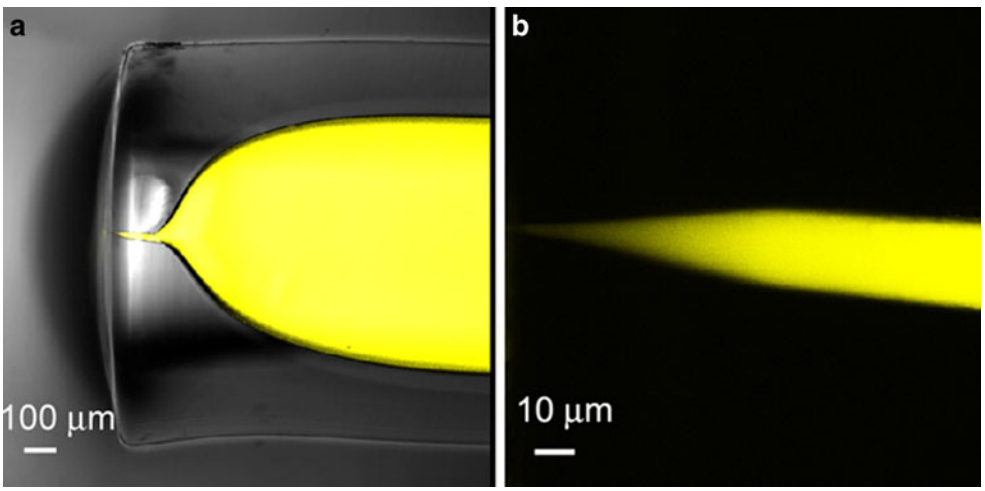

Fig. 1 Profiles of a single conical nanopore channel in glass capillary filled with 100 μmol/L R6G water solution (with 340 nm orifice radius). **a** Overlay of bright-field and fluorescence images of the conical nanopore channel in the capillary, 10×objective (NA 0.4). **b** Fluorescence image of the conical nanopore channel, 20×objective (NA 0.7). Here the capillary was placed horizontally on the specimen stage of the microscope

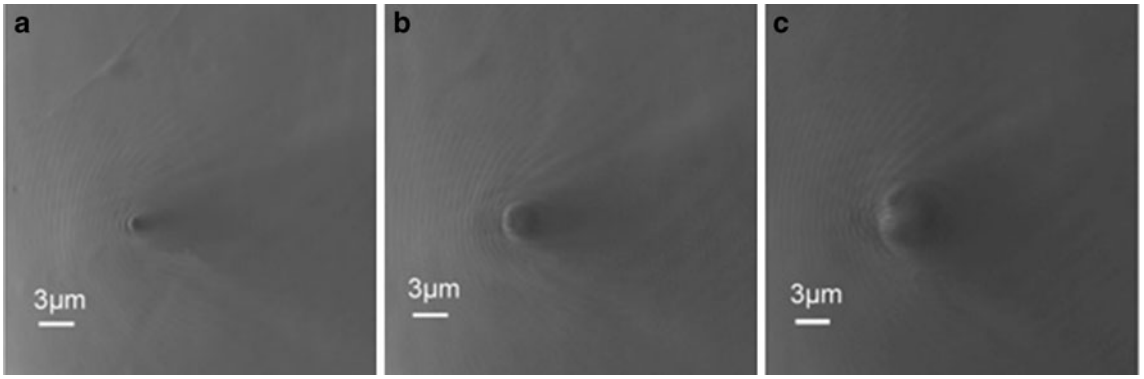

Fig. 2 Bright-field images of a single conical glass conical nanopore channel at different depths (with 340 nm orifice radius) **a** Near the orifice (at ~500 nm radius) **b** 7 μm from the orifice (at 1 μm radius) **c** Near the bottom, 17 μm from the orifice (at 2 μm radius). Here the channel was placed vertically on the specimen stage of the microscope,100×objective (NA 1.4)

immersion objective were used. Different optical sections of the conical nanopore channel were obtained. Emission wavelength range was 550-650 nm. Step size and band width were 3 nm and 10 nm respectively.

Fluorescence Recovery after Photobleaching (FRAP) in Conical Nanopore Channel In FRAP, 1,400 Hz line frequency scan speed with bidirectional scan was used. In combination with an image format of 256×256 pixels, one image every 203 ms can be recorded. Pinhole size was set to 2 airy units (121 μm). The excitation source was an argon ion laser, wavelength 488 nm and a 20× (NA 0.7) objective was used. Initial intensity images were taken over several the regions of interest (ROIs, an ellipse region with an aera about 75 μm^2) along a conical nanopore channel filled with 100 μmol/L FITC 20% glycerol water solution for 1.05 s (10% of the bleach intensity), then the laser power was increased to 100% and the ROI regions were photo-bleached for 40.6 s. The fluorescence recovery of the bleached areas was monitored by reducing the laser power (10% of the bleach intensity) and recording images every 1 s for 100 s.

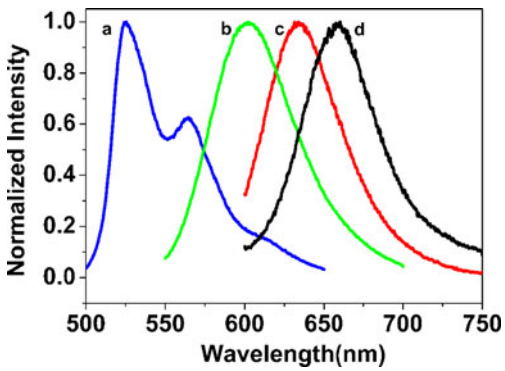

Fig. 3 Fluorescence emission spectra of Nile red in different solvents: n-hexane (a), ethyl acetate (b), methanol (c) and water (d)

Results and Discussion

The capillary was placed on a coverslip with the nanopore end directly over the objective. Then, several drops of a refractive index matching oil (n=1.51) were used to immerse the capillary to reduce refraction and scattering from the capillary walls, thus obtaining an undistorted image. Figure 1 shows the profile of a conical nanopore channel filled with 100 μmol/L R6G solution and Fig. 2 shows the vertical section at different depth of a glass conical nanopore channel.

Nile red is one of the most popular fluorescent probes, because the fluorescence properties of this molecule highly depend on the polarity of the surrounding environment, and it has shown to be an excellent fluorescence probe for the environmental diversity in biological and micro heterogeneous systems [26].

The emission spectra of Nile red (Fig. 3) in bulk solution were examined in a series of polar and non-polar

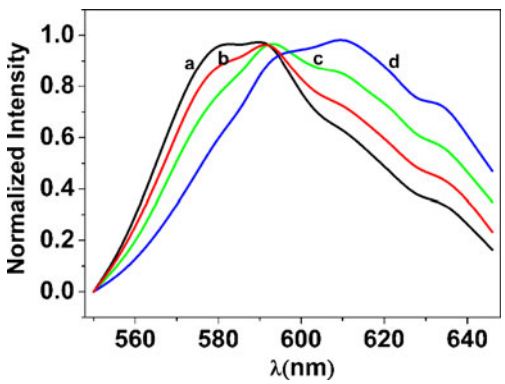

Fig. 4 Confocal fluorescence spectra of 20 μmol/L Nile red ethyl acetate solution at different optical sections of a single conical channel (~50 nm orifice radius). Spectra were obtained at radius of ~50 nm (a), ~210 nm (b), ~520 nm (c) and ~1.6 μm (d), respectively. The capillary was placed vertically on the specimen stage of the microscope to obtain different optical sections of the channel. 20×objective(NA 0.7) was used

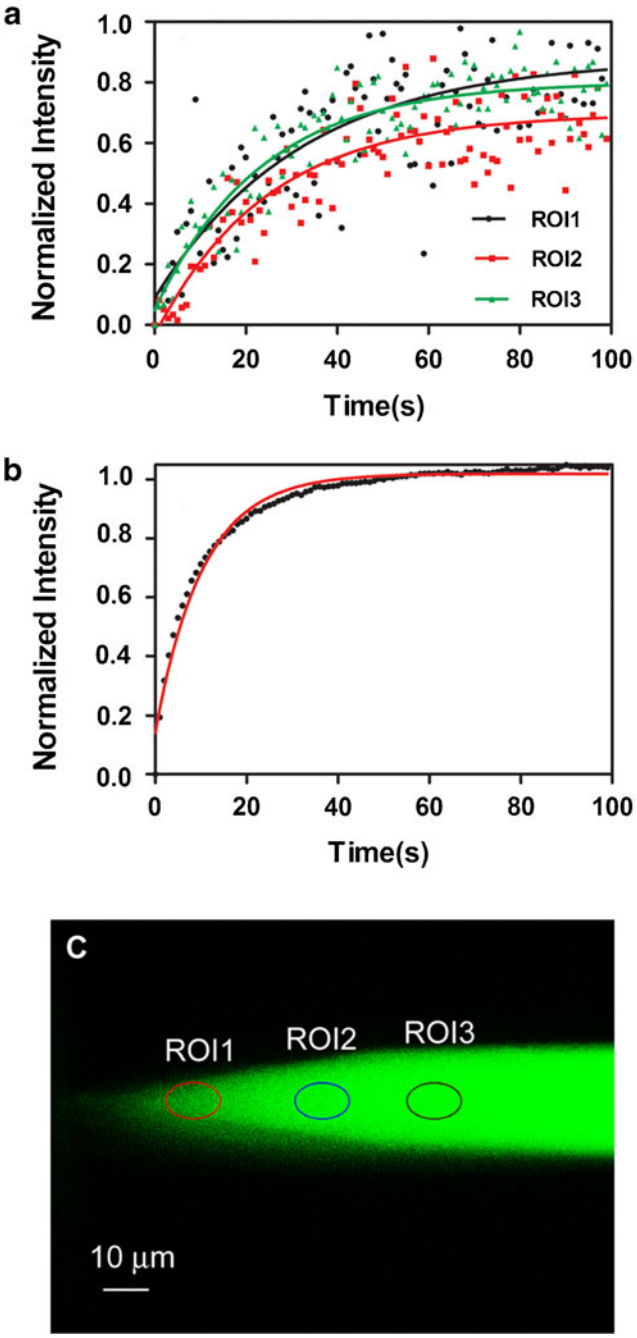

Fig. 5 **a** Fluorescence recovery curves of the chosen ROIs (an area about 75 μm^2, at radius of 3, 7, 10 μm, respectively) in a conical nanopore channel (with 340 nm orifice radius) filled with 100 μmol/L FITC 20% glycerol water solution. **b** Fluorescence recovery curve of bulk solution. **c** The positions of the ROIs in the channel chosen for FRAP experiments

solvents by a laboratory constructed fluorescence spectrophotometer [27–30]. In water, methanol, ethyl acetate and n-hexane, the maximum emission wavelengths were 663, 633, 602, 526 nm respectively. Increasing polarity leads to a substantial red shift of the emission maxima.

We used Nile red to gauge the local environmental differences in the channel. Optical sections are taken along the nanopore (moving from smaller to larger radii) and the corresponding fluorescence spectra at each section are obtained. The result shows a red shift of the emission spectra is observed from the tip section to the bottom section (as seen in Fig. 4). The closer the fluorescence molecules near the tip region, the greater the number of surface-adsorbed dye molecules, thus may leading to the prominent spectra shift of the fluorescence emission spectra.

The solvatochromic behavior observed arises from the fact that Nile red undergoes large dipole moment of the molecules in the excited state and the existence of a non-emissive twisted intramolecular charge transfer (TICT) state, which is more likely to be formed in polar than nonpolar environments [31–35]. The spectra diversities of Nile red may indicate the nonpolar to polar environment transfer in the channel.

Fluorescence recovery after photobleaching (FRAP) was used to monitor diffusion of dye molecules Fluorescein isothiocyante (FITC) in conical nanopore channels. In a typical FRAP experiment, an intense laser light is used to photobleach fluorophores in a small ROI, following which the recovery of the fluorescence, due to the diffusion of unbleached fluorophores into the ROI, is monitored with a highly attenuated laser beam, thus diffusion rate of fluorescent molecules is determined locally directly in the microscope.

Figure 5a and b shows the fluorescence recovery curves of the FRAP experiments performed in a channel (filled with 100 μmol/L FITC 20% glycerol water solution) and the bulk solution respectively. Figure 5c shows the confocal fluorescence image of a conical nanopore channel and the positions of ROIs chosen for FRAP experiments. The capillary was placed horizontally on the specimen stage of the microscope, and the ellipse regions indicated the ROIs at radius of 3, 7, 10 μm, respectively) chosen for photobleaching.

Table 1 Results from fluorescence recovery after photobleaching (FRAP) experiments

	ROI_1	ROI_2	ROI_3
Orifice Radius 50 nm			
position(radius, μm)	3	7	10
$t_{1/2}$ (s)	22.4	17.1	16.3
D (cm^2/s)	1.07×10^{-7}	1.40×10^{-7}	1.47×10^{-7}
Orifice radius 872 nm			
position(radius, μm)	2	5	7.5
$t_{1/2}$ (s)	52.0	22.4	16.1
D (cm^2/s)	4.61×10^{-8}	1.07×10^{-7}	1.49×10^{-7}

For a system containing a single diffusible species, the fluorescence intensity increases as a function of time after the bleach pulse due to diffusion of molecules into the area probed by the beam. The time it takes for the curve to reach 50% of the plateau fluorescence intensity is called 'half maximum' or 'half life' and often abbreviated as '$t_{1/2}$', and is calculated from a normalized single exponential association fitting of the recovery curve according to Eq. 2 [36].

$$I(t) = A(1 - e^{-k \cdot t}) \tag{2}$$

Where I refer to the fluorescence intensity, A is the fluorescence intensity in the bleached region after full recovery (mobile fraction), k is the diffusion rate constant and t is the diffusion time. The half life is calculated after fitting with Eq. 3:

$$t_{1/2} = \frac{\ln 2}{k} \tag{3}$$

The calculated $t_{1/2}$ of the ROI_1, ROI_2, ROI_3 were 22.4, 17.1, 16.3 s respectively, and the $t_{1/2}$ of bulk solution was 7.21 s. It indicates that dye diffusion confined in the nanopore channel is much slower than that of in the bulk solution and varied with the different positions in the channel. Rate of diffusion was determined by the diffusion constant of the molecule, which is affected by the size of the molecule, viscosity and temperature of the surrounding medium. The diffusion coefficient (D) was finally calculated using Eq. 4.

$$D = \frac{0.88\omega^2}{4t_{1/2}} \tag{4}$$

(ω is the $1/e^2$ Gaussian radius.). The calculated diffusion coefficients of the ROI regions in the channel were 1.07×10^{-7}, 1.40×10^{-7}, 1.47×10^{-7} cm^2/s respectively, while the calculated diffusion coefficients was 3.32×10^{-7} cm^2/s in bulk solution. Table 1 gives the results of the FRAP experiments performed in conical channels with different orifice radius.

The results show that dye diffusion confined in a conical nanopore channel was much slower than that of the bulk solution and varied with the different positions in the channel, which indicated that the interior of the channel was heterogeneous in terms of diffusion. Diffusion was slower in the tip and faster at the bottom of the channel.

Conclusions

In summary, we performed the first experiment to explore the local environmental differences between the behavior of molecules in the bulk of the fluid and molecules confined in pores by the integration of conical nanopore channel with CLSM. The fluorescence emission spectra of Nile red show a red shift from the tip to the bottom of the conical channel, indicating that the confinement of nanochannel on the fluorescence properties of molecules. FRAP experiments of FITC revealed that the diffusion of dye molecules being confined in single conical nanopore channel is slower than that in the bulk solution, and the diffusion rates depended on their positions in the channels. Single conical nanopore channels provide potential possibilities for studying physical or chemical processes occurring in nanoconfinement in situ.

Acknowledgments We are grateful for the financial support from the National Natural Science Foundation of China (20975084, 20575055), the National Basic Research Program of China (973Program, 2007CB935600) and the Science and technology program of Fujian Province (2009Y0046). We thank Professor Richard N. Zare for the illumination in applications of nanopores, and Professor Henry S. White and his coworkers for sharing the experience of glass nanopore fabrication.

References

1. Choi Y, Baker LA, Hillebrenner H, Martin CR (2006) Biosensing with conically shaped nanopores and nanotubes. Phys Chem Chem Phys 8:4976–4988
2. Gyurcsanyi RE (2008) Chemically-modified nanopores for sensing. TrAC Trends Anal Chem 27:627–639
3. Howorka S, Siwy Z (2009) Nanopore analytics: sensing of single molecules. Chem Soc Rev 38:2360–2384
4. Gardeniers HJGE (2009) Chemistry in nanochannel confinement. Anal Bioanal Chem 394:385–397
5. Bohrer MP, Patterson GD, Carroll PJ (1984) Hindered diffusion of dextran and ficoll in microporous membranes. Macromolecules 17:1170–1173
6. Ladero M, Santos A, Garcia-Ochoa F (2007) Hindered diffusion of proteins and polymethacrylates in controlled-pore glass: An experimental approach. Chem Eng Sci 62:666–678
7. Turner SWP, Cabodi M, Craighead HG (2002) Confinement-induced entropic recoil of single DNA molecules in a nanofluidic structure. Phys Rev Lett 88:128103/1–128103/4
8. Tang J, Trahan DW, Doyle PS (2010) Coil-stretch transition of DNA molecules in slitlike confinement. Macromolecules 43:3081–3089
9. Reisner W, Morton KJ, Riehn R, Wang YM, Yu Z, Rosen M, Sturm JC, Chou SY, Frey E, Austin RH (2005) Statics and dynamics of single DNA molecules confined in nanochannels. Phys Rev Lett 94:196101/1–196101/4
10. Ulrich K, Galvosas P, Kaerger J, Grinberg F, Vernimmen J, Meynen V, Cool P. Self-assembly and diffusion of block copolymer templates in sba-15 nanochannels. J Phys Chem B 114: 4223–4229
11. Mobius W, Frey E, Gerland U (2008) Spontaneous unknotting of a polymer confined in a nanochannel. Nano Lett 8:4518–4522
12. Yu B, Sun P, Chen T, Jin Q, Ding D, Li B, Shi A-C (2007) Self-assembled morphologies of diblock copolymers confined in nanochannels: Effects of confinement geometry. J Chem Phys 126:204903/1–204903/5

13. Sorin EJ, Pande VS (2006) Nanotube confinement denatures protein helices. J Am Chem Soc 128:6316–6317
14. Moorthy J, Burgess R, Yethiraj A, Beebe D (2007) Microfluidic based platform for characterization of protein interactions in hydrogel nanoenvironments. Anal Chem 79:5322–5327
15. Hibara A, Saito T, Kim H-B, Tokeshi M, Ooi T, Nakao M, Kitamori T (2002) Nanochannels on a fused-silica microchip and liquid properties investigation by time-resolved fluorescence measurements. Anal Chem 74:6170–6176
16. De Santo I, Causa F, Netti PA (2010) Subdiffusive molecular motion in nanochannels observed by fluorescence correlation spectroscopy. Anal Chem 82:997–1005
17. Sexton LT, Horne LP, Martin CR (2007) Developing synthetic conical nanopores for biosensing applications. Mol Biosyst 3:667–685
18. Gierschner J, Egelhaaf HJ, Mack HG, Oelkrug D, Alvarez RM, Hanack M (2003) Luminescence of conjugated molecules confined in nanochannels. Synth Met 137:1449–1450
19. Kievsky Y Y, Carey B, Naik S, Mangan N, ben-Avraham D, and Sokolov I (2008) Dynamics of molecular diffusion of Rodamine 6 G in silica nanochannels. *J. Chem. Phys.* 128: 151102/1–151102/5.
20. Oh Y-J, Garcia AL, Petsev DN, Lopez GP, Brueck SRJ, Ivory CF, Han SM (2009) Effect of wall-molecule interactions on electrokinetic transport of charged molecules in nanofluidic channels during FET flow control. Lab Chip 9:1601–1608
21. Wang G, Zhang B, Wayment JR, Harris JM, White HS (2006) Electrostatic-gated transport in chemically modified glass nanopore electrodes. J Am Chem Soc 128:7679–7686
22. Cao X-H, Zhang L-X, Cai W-P, Li Y-Q (2010) Amperometric sensing of dopamine using a single-walled carbon nanotube covalently attached to a conical glass micropore electrode. Electrochem Commun 12:540–543
23. Weiss AM, Saraidarov T, Reisfeld R (2001) Confocal microscopy for characterization of porous sol-gel glasses incorporating luminescent dyes. Opt Mater 16:15–20
24. Zhang B, Galusha J, Shiozawa PG, Wang G, Bergren AJ, Jones RM, White RJ, Ervin EN, Cauley CC, White HS (2007) Bench-top method for fabricating glass-sealed nanodisk electrodes, glass nanopore electrodes, and glass nanopore membranes of controlled size. Anal Chem 79:4778–4787
25. Zhang B, Zhang Y, White HS (2006) Steady-state voltammetric response of the nanopore electrode. Anal Chem 78:477–483
26. Cser A, Nagy K, Biczok L (2002) Fluorescence lifetime of Nile Red as a probe for the hydrogen bonding strength with its microenvironment. Chem Phys Lett 360:473–478
27. Lin D-L, He L-F, Li Y-Q (2004) Rapid and simultaneous determination of coproporphyrin and protoporphyrin in feces by derivative matrix isopotential synchronous fluorescence spectrometry. Clin Chem 50:1797–803
28. Zhou P-C, Huang W, Zhang R-B, Zou Z-X, Luo H-D, Falih AA, Li Y-Q (2008) A simple and rapid fluorimetric method for simultaneous determination of protoporphyrin ix and zinc protoporphyrin ix in whole blood. Appl Spectrosc 62:1268–1273
29. Chen Z, Tang YJ, Xie TT, Chen Y, Li YQ (2008) Fluorescence spectral properties of rhodamine 6 g at the silica/water interface. J Fluoresc 18:93–100
30. Tang YJ, Chen Y, Yao MN, Zou ZX, Han GB, Li YQ (2008) Total internal reflection fluorescence spectroscopy for investigating the adsorption of a porphyrin at the glass/water interface in the presence of a cationic surfactant below the critical micelle concentration. J Fluoresc 18:261–267
31. Hungerford G, Ferreira JA (2001) The effect of the nature of retained solvent on the fluorescence of nile red incorporated in sol-gel-derived matrices. J Lumin 93:155–165
32. Krishna MMG (1999) Excited-state kinetics of the hydrophobic probe nile red in membranes and micelles. J Phys Chem A 103:4129
33. Datta A, Mandal D, Pal SK, Bhattacharyya K (1997) Intramolecular charge transfer processes in confined systems. Nile red in reverse micelles. J Phys Chem B 101:10221–10225
34. Dutta AK, Kamada K, Ohta K (1996) Spectroscopic studies of nile red in organic solvents and polymers. J Photochem Photobiol A 93:57–64
35. Stuart MCA, van de Pas JC, Engberts JBFN (2005) The use of nile red to monitor the aggregation behavior in ternary surfactant-water-organic solvent systems. J Phys Org Chem 18:929–934
36. Hungerford G, Rei A, Ferreira MIC, Tregidgo C, Suhling K (2007) Molecular diffusion within sol-gel derived matrices viewed via fluorescence recovery after photobleaching. Photochem Photobiol Sci 6:825–828